

# BUCKLING OF BEAMS WITH INFLECTION POINTS

*Joseph A. Yura<sup>1</sup> and Todd A. Helwig<sup>2</sup>*

## ABSTRACT

The buckling behavior of beams with reverse curvature bending can be complex since both flanges are subjected to compression at different locations along the unbraced length. Design engineers frequently raise questions regarding the inflection point behaving as a braced point in continuous construction. The problem is further complicated when the top flange is braced by closely-spaced joists or composite construction while the bottom flange is unbraced. Although the moment is zero at the inflection point, the location can not generally be treated as a braced point because the section can still twist at this location. A variety of commonly encountered design problems are discussed and simple solutions are provided in the form of  $C_b$  factors applied to the uniform moment solution. The problems that are considered include beams with reverse curvature bending with no intermediate bracing, as well as members with continuous bracing on the top flange. For members with bracing on one flange, solutions are presented for lateral bracing, torsional bracing and composite construction.

---

<sup>1</sup> Professor Emeritus, Department of Civil, Arch. and Env. Engineering, The University of Texas at Austin, Austin, TX 78712

<sup>2</sup> Associate Professor, Department of Civil, Arch. and Env. Engineering, The University of Texas at Austin, Austin, TX 78712

## **INTRODUCTION**

Two of the primary factors that affect the lateral-torsional buckling capacity of a beam are the unbraced length and the distribution of bending moment along the member. Effects of moment gradient are usually accounted for by adjusting the buckling solution derived for uniform moment loading. However, when addressing the unbraced length, engineers are often unsure what constitutes a braced point. This is particularly true for beams with inflection points due to reverse curvature bending. Since the moment is zero at the inflection point, questions frequently arise regarding this point behaving as a braced point (AISC-1993, 1995, CISC, 2003). In many of these situations the top flange of the girder may be laterally braced by a flooring system or joists, while the bottom flange is unbraced.

As the name implies, the lateral-torsional buckling mode of beams involves both lateral translation and twist of the cross section. Bracing that restrains one point on the cross section from lateral movement does not ensure adequate bracing. However, preventing twist of the cross section ensures that the point is braced (Yura, 1993). This paper focuses on the buckling behavior of beams with inflection points. Background information is presented in the next section followed by finite element results on beams with reverse curvature bending. Several bracing scenarios with reverse curvature bending are considered, ranging from cases with no intermediate bracing to situations with lateral bracing on one flange only. Expressions for  $C_b$  factors that reflect the beneficial effects of the bracing are presented and discussed.

## **BACKGROUND**

Most design specifications employ lateral-torsional buckling solutions that were developed for constant bending moment and account for variable moment with  $C_b$  factors applied to the uniform moment

solution. For doubly-symmetric sections with uniform moment loading ( $C_b = 1.0$ ), the elastic buckling moment (Timoshenko and Gere, 1961) is

$$M_{cr} = C_b \frac{\pi}{L_b} \sqrt{EI_y GJ + \left(\frac{\pi E}{L_b}\right)^2 I_y C_w} \quad (1)$$

where  $L_b$  = unbraced length,  $E$  = modulus of elasticity,  $G$  = shear modulus,  $J$  = torsional constant,  $I_y$  = weak axis moment of inertia and  $C_w$  = warping constant. The first term under the radical in Eq.1 relates to the St. Venant torsional stiffness, while the second term within the radical reflects the warping stiffness of the beam. In the derivation of Eq.1, only the boundary conditions that twist was prevented at the ends of the unbraced length and no warping restraint at the ends were used. No lateral displacement boundary condition was necessary. Thus, locations along the length of the member where twist is prevented are defined as brace points, For beams with moment gradient, Kirby and Nethercot (1979) presented a general expression for  $C_b$  that is applicable to a variety of moment diagram shapes within the unbraced length. Their equation was adjusted slightly and is presented in the American Institute of Steel Construction Specification (AISC, 2005) in the following form:

$$C_b = \frac{12.5M_{max}}{2.5M_{max} + 3M_A + 4M_B + 3M_C} \quad (2)$$

where, within the unbraced beam segment,  $M_{max}$  = maximum moment,  $M_A$ ,  $M_C$  = moments at the quarter points and  $M_B$  = moment at the center. The absolute values of all moments are used with Eq. 2.

The unbraced length to be used with Eq.1 for beams with inflection points can be misinterpreted, especially if the definition of  $L_b$  in design specifications refers to the unbraced length of the *compression flange*. Since the inflection point defines the switch from compression to tension in the flange, can the inflection point be used to define  $L_b$ ? The inflection point generally does not act as a braced point since the

beam can still twist at this location as shown in Fig.1, which depicts the buckled shape of a beam with equal and opposite end moments with twist prevented at the ends. The asymmetric loading causes an inflection point at midspan. The figure shows a plan view of the buckled shape of the top and bottom flanges along the length of the beam. Although the lateral displacement at midheight of the cross section is zero at the inflection point, the top and bottom flanges have equal and opposite lateral displacements resulting in a pure twist of the cross section.

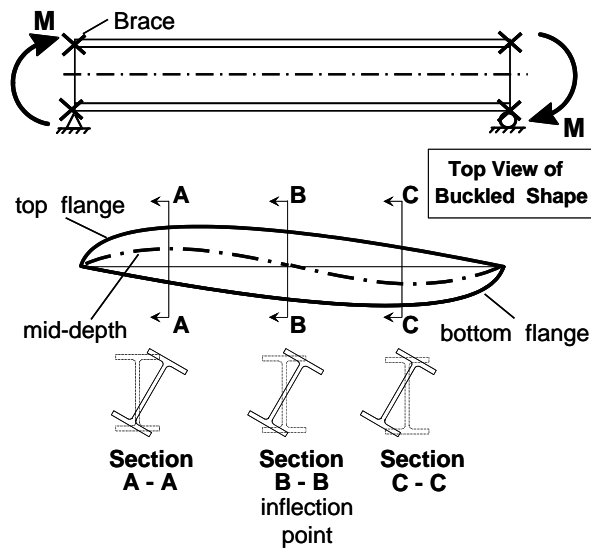


Fig. 1. Twist at the Inflection Point

A common misconception when dealing with reverse curvature bending is that a flange in tension does not displace laterally and therefore the inflection point can be assumed to act as a braced point. The tensile regions of the flanges do remain relatively straight during buckling, but Fig.1 shows that they displace laterally and allow the section to twist. Therefore, the inflection point does not behave as a braced point since the cross section can still twist at this location. A

single lateral brace attached to just one of the flanges at the inflection point also does not prevent twist and only increases  $M_{cr}$  approximately 10% (Yura, 1993). Bracing both flanges at the inflection point more than doubles the value of  $M_{cr}$ .

A design approach that is consistent with current design provisions is to define the unbraced length as the spacing between points of zero twist, and to account for effects of the inflection points with  $C_b$  factors applied to a uniform moment buckling solution. The remainder of this paper will therefore focus on  $C_b$  expressions for frequently encountered details that affect a beams buckling capacity. Finite element solutions (FEA) are presented in the paper for a variety of loading conditions. The cross section that was used in the majority of the analyses was a W16x26 section with a span-to depth ratio,  $L/d$ , of 15 and 30.

## UNBRACED BEAMS

Lateral-torsional buckling strength can be determined by using the  $C_b$  expression give by Eq. 2 provided that the unbraced length is defined between points of zero twist. The buckling moment is compared to the maximum applied moment within the unbraced length under consideration. Eq. 2 is valid for both single- and reverse-curvature bending of doubly-symmetric sections and is applicable for any shape moment diagram between points of zero twist.

The accuracy of Eq. 2 with FEA solutions are presented in Fig. 2 for a W16x26 beam with a distributed load applied at the centroid. The beam was subjected to similar concentrated in-plane moments at the two ends to simulate continuity. Although no intermediate bracing was provided along the length of the beam, twist was prevented at the ends of the beam. Since the beams were free to warp at the supports, the results will be conservative for continuous construction. The  $C_b$  is graphed on the vertical axis versus the ratio of the midspan moment,  $M_{CL}$ , to the end moment,  $M_{END}$ . Eq. 2 has good agreement with the FEA results over the wide range of moment distributions that were

considered. The expression is conservative when the midspan moment is small relative to the end moment, which is a complicated region of behavior. The two different FEA curves in this region show that there is a relatively large variability in the  $C_b$  value depending on the span/depth ratio,  $L/d$ . Similar results were obtained when one end moment was zero. Eq. 2 has also been shown to be accurate for beams with concentrated loads and linear moment diagrams (Yura, 1987). In general, Eq. 2 provides good estimates of  $C_b$  for both single and reverse curvature bending.

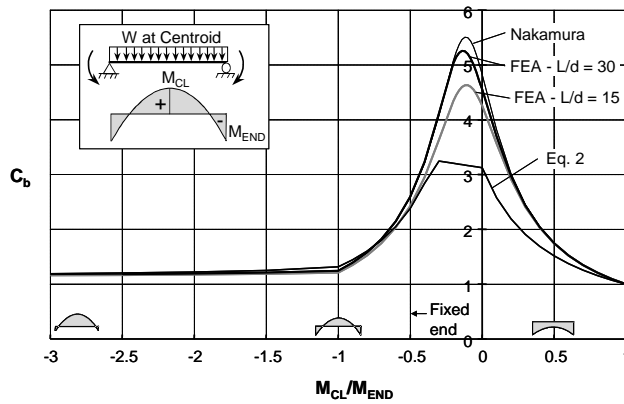


Fig. 2. Unbraced Gravity Loaded Beam with Restrained Ends

Nakamura and Wakabayashi (1981) derived a general expression for  $C_b$  from basic principles for beams with uniformly distributed load and restraining end moments. Their  $C_b$  formulation is more complex because it includes load height effects and lateral bracing. The Nakamura-Wakabayashi solution and the FEA results compare very favorably for the loading case in Fig. 2.

The FEA results in Fig. 2 show that for a negative  $M_{CL}/M_{END}$  ratio (positive midspan moment),  $C_b$  increases substantially as the midspan moment gets smaller. The moment at midspan is a dominating buckling factor. This observation leads to a simple approach for estimating the

buckling load for unbraced gravity-loaded beams with restrained ends; use  $C_b = 1.14$  with the midspan moment, even if the midspan moment is smaller than the end moment. The accuracy of this simple method is demonstrated in Fig. 3 for beams with uniform load and restrained at one or both ends. The limiting ratios of  $M_{END}/M_{CL} = 0$  and  $-2$  correspond to pinned ends and fixed end(s), respectively.  $C_b$  derived from the FEA results for the two cases are shown by the two solid lines.  $C_b = 1.14$  is shown dashed. For the propped cantilever the comparison between FEA and  $C_b = 1.14$  is almost exact over the entire practical range of end restraint. For the propped cantilever the midspan moment is smaller than the maximum positive moment so it would be conservative to use the maximum moment near midspan. For both ends restrained, the simple approach is slightly conservative ( $< 7\%$ ).

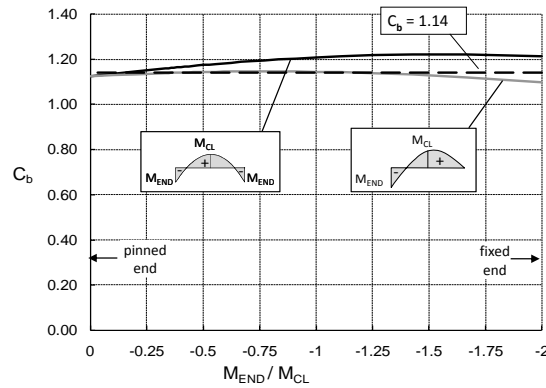


Fig. 3. Simplified Method for Unbraced Gravity-Loaded Beams

### GRAVITY-LOADED BEAMS BRACED ON TOP FLANGE

In the previous section on unbraced beams, gravity load was applied at the centroid of the cross section. Theoretically, in unbraced gravity-loaded I-shaped beams with  $L/d = 15$ , top flange loading on a simple

span reduces the buckling load 30% (Nethercot and Rocky, 1972). When there are inflection points between the brace points, the load height effect is greater: 45% for a propped cantilever (one inflection point) and 60% for a fixed-end beam (two inflection points). For longer beams, the load height effect is less significant than for shorter spans. Top flange loading was not considered previously because the loading system typically also provides bracing at the location where the load is applied. In this section, however, the top flange is braced continuously so gravity loading will also be applied at the top flange. The  $C_b$  factors generated are applied to Eq. 1 unless otherwise noted. The  $C_b$  factor accounts for the effects of moment gradient, top flange loading and top flange bracing.  $L_b$  will be the unbraced length of the bottom flange.

There are three general types of bracing that improve the buckling strength of I-shaped beams: lateral bracing, torsional bracing and diaphragm bracing. Lateral bracing prevents lateral movement at the point on the cross section where the brace is attached. When applied to only one flange in a beam with inflection points, lateral bracing will not prevent lateral-torsional buckling, but the buckling capacity will be improved. Torsional bracing prevents twist of the cross section at the point of attachment, but lateral movement can occur. However, because the web of an I-shaped beam is relatively thin, cross-section distortion must be considered in evaluating the effectiveness of the brace. Stiffeners can be used at the brace point to eliminate the web distortion. Diaphragm bracing, such as a deck form attached directly to the beam flange, increase the lateral buckling capacity by providing warping restraint to the flange that tends to keep the flange straight. Attachment details must be considered when evaluating the effectiveness of deck forms.

A more detailed discussion of the three bracing types, along with minimum strength and stiffness requirements for design, can be found elsewhere (Yura, 1993, Helwig and Yura, 2008). For the solutions contained herein, lateral bracing will be assumed sufficiently stiff to prevent any lateral movement of the top flange. For torsional bracing it is assumed that the top flange has zero twist. Functionally, lateral and

diaphragm bracing both resist lateral bending of the flange so only lateral and torsional bracing will be considered. During erection and construction, one or more of the three components may be available to stabilize the beam. For example, joists or purlins alone framing between adjacent beams can provide a small amount of torsional restraint (Essa and Kennedy, 1995). When decking is attached to the joists, lateral displacement of the top flange will also be prevented at the joist locations. Usually the torsional restraint is ignored in this case. In composite construction both lateral movement and twist of the top flange are prevented. In the following subsections,  $C_b$  expressions suitable for design are developed from finite element buckling analyses that can account for cross-section distortion. Loading conditions that produce one or two inflection points within the unbraced bottom flange are discussed.

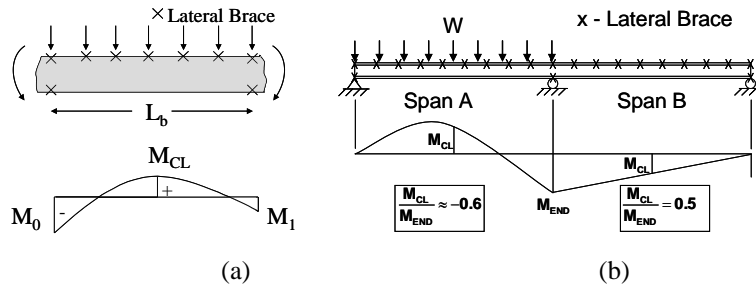


Fig. 4. Restrained Beams with Top Flange Lateral Bracing

**Lateral Bracing.** For restrained beams laterally braced along the top flange as shown in Fig. 4a, the bottom flange is subjected to compression along the unbraced length, which makes the beam susceptible to lateral-torsional buckling. Numerous buckling analyses were performed on single spans with the ends prevented from twisting and with zero end warping restraint. Most analyses were performed on 20 and 40 ft long W16×26 sections that have one of the highest web

slenderness ratios for rolled shapes. This was done to maximize the potential distortion so the conservative results would be applicable to all W-shapes. Based on the FEA results, the following  $C_b$  expression was developed for design:

$$C_b = 3.0 - \frac{2}{3} \left( \frac{M_1}{M_o} \right) - \frac{8}{3} \frac{M_{CL}}{(M_o + M_1)^*} \quad (3)$$

\*Take  $M_1 = 0$  in this term if  $M_1$  is positive.

where  $M_o$  = moment causing the largest bottom flange compressive stress at the end of the unbraced length,  $M_1$  = other end moment and  $M_{CL}$  = moment at the middle of the unbraced length. The (\*) in Eq. 3 indicates that  $M_1$  should be taken as zero in the last term if it does not cause compression in the bottom flange. The sign convention for Eq.3 is denoted in Fig.4a with negative moments causing compression in the bottom flange. The  $C_b$  from Eq. 3 is used with Eq. 1 to determine the critical moment to be compared to  $M_o$ . Yielding must also be checked with the largest moment.

Fig. 4b depicts a potential load case and distribution of moment for a continuous beam. Although the beam has continuous lateral bracing on the top flange, twist is prevented only at the supports and therefore the span length of Spans A and B would be used for the unbraced lengths along with the  $C_b$  factor from Eq. 3. Since one end of both spans are pinned,  $M_1=0$  in Eq. 3, while  $M_o=M_{END}$ . The values of  $M_{CL}$  in this case would simply be the moment at the middle of the span under consideration. The applicability of Eq. 3 will be demonstrated for three general cases: straight line moment diagrams, and gravity loaded beams with one and two inflection points.

A graph of Eq. 3 is compared to FEA solutions for straight line moment diagrams with various ratios of  $M_1/M_o$  in Fig. 5. The straight line moments depicted on the horizontal axis could be the result of loading cases that cause the moments shown for Span B in Fig. 4b or from beam moments caused by lateral frame loads. The graph of Eq. 3 has a change in slope for negative ratios of  $M_1/M_o$ , because  $M_1$  is taken

as zero in the last term of Eq. 3 when it does not cause compression in the bottom flange. Fig. 5 shows that the  $C_b$  values become large when the length of the bottom flange subjected to compression becomes relatively small: however, the unbraced length is always taken as the spacing between points of zero twist. In general, Eq. 3 has good agreement with the results from the FEA analysis for for both  $L/d$  values. For  $L/d = 30$ , yielding at  $M_t$  will control the design when  $C_b$  is approximately 6, which corresponds to  $M_1/M_0 = -2$ . If Eq. 2 is used to estimate the lateral buckling strength, the results will be satisfactory when the entire bottom flange is in compression ( $M_1/M_0 > 0$ ). With loading causing an inflection point, Fig. 5 shows that the use of Eq. 2 will produce very conservative designs.

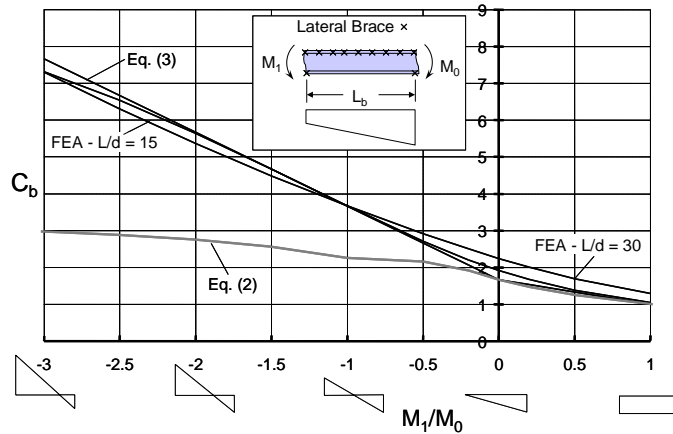


Fig. 5. Top Flange Laterally Braced - Linear Moment Diagram

A restrained beam with one end pinned and uniform gravity load on the span as illustrated in Span A of Fig. 4 will typically have one inflection point. The end moment was held constant while the distributed load was changed to achieve various ratios of  $M_{CL}/M_{END}$ . With this distributed load arrangement, top flange loading effects will be present. Buckling solutions are shown in Fig. 6. Moment diagrams

along the horizontal axis depict the distribution of moment along the beam length. Although there is a slight amount of reverse curvature for the case of  $M_{CL}/M_{END} = 0$ , results to the right of the ordinate generally represent the behavior of single curvature bending causing compression in the unbraced flange while results to the right of the ordinate represent reverse curvature bending. The  $C_b$  factors from both Eqs. 2 and 3 are shown along with FEA results for  $L/d$  of 15 and 30. For the case of single curvature bending ( $M_{CL}/M_{END} > 0$ ), there is very little difference among Eq. 2, Eq. 3 and the FEA results. This demonstrates that tension flange bracing has very little impact on the buckling solution. However for cases with reverse curvature, Eq. 2 significantly underestimates the buckling capacity. Top flange loading is the principal factor for the separation between the FEA results for  $L/d = 15$  and 30. Eq. 3 is in good agreement with  $L/d = 15$  results and is conservative for the longer span. Most practical continuous beams will be in the  $L/d$  range of 25~30 and although Eq. 3 is conservative, the slope of the line follows the general trend of the FEA curves for the full range of moments considered.

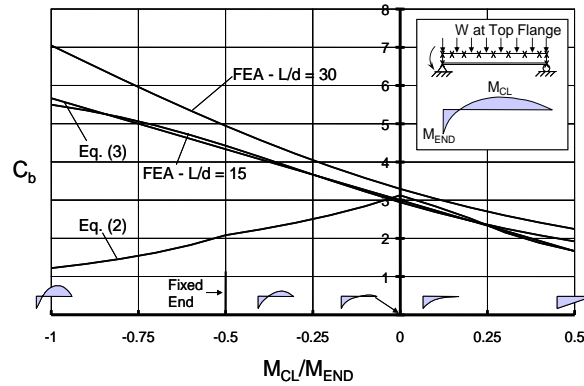


Fig. 6. Top Flange Laterally Braced – One End Restrained

Beams with similar in-plane restraints at both ends will have two inflection points within the unbraced length. Solutions for this case are

given in Fig. 7. For  $0 < M_{CL}/M_{END} < 1$ , the bottom flange is entirely in compression and the exact  $C_b$  values that range between 1.0 and 2.3 are affected by the  $L/d$  ratio. Within this range of  $M_{CL}/M_{END}$ , Eq. 3 is accurate for  $L/d=30$  but is unconservative for  $L/d=15$ . However, cases within this range of  $M_{CL}/M_{END}$  are not too common. Most typical cases are those in the range of  $-1.0 < M_{CL}/M_{END} < -0.5$  as indicated by the label “practical range” on the graph. In these cases the bottom flange compression region is confined near the ends of the beam.  $C_b$  values greater than 3.0 are encountered for  $M_{CL}/M_{END} < -0.5$ . A comparison of Figs. 6 and 7 shows that lateral buckling is more critical for the case with two inflection points (smaller  $C_b$  for the same  $M_{CL}/M_{END}$ ). The buckled shapes always show that the maximum lateral displacement occurs at midspan where the bottom flange is in tension so a single bottom flange lateral brace at midspan can substantially increase the lateral buckling capacity. It will be shown later that a small amount of torsional restraint typically available in lateral bracing systems mitigates the unconservatism shown in Fig. 7.

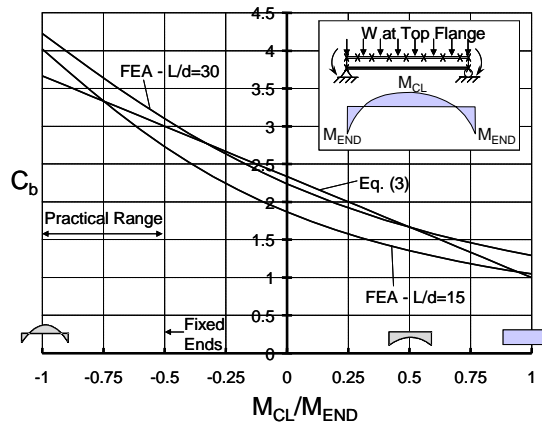


Fig. 7. Top Flange Laterally Braced – Both Ends Restrained

**Torsional Bracing.** A torsional bracing system resists twisting of the beam. Lateral displacement at the brace point can still occur. Properly designed cross frames or diaphragms framing between adjacent beams

act as torsional braces because they prevent beam twisting at those locations. When the torsional brace is attached to either flange or just a portion of the web depth, web cross-sectional distortion can occur that diminishes the effectiveness of the torsional brace. Yura (1993) has presented the following expression for the buckling strength of a torsionally braced beam that accounts for the distortion,  $M_T$ , based on the solution developed by Taylor and Ojalvo (1966):

$$M_T = \sqrt{C_{bu}^2 M_{cr}^2 + \frac{C_{bb}^2 \bar{\beta}_T E I_y}{C_T}} \quad (4)$$

$C_{bu}$  and  $C_{bb}$  are the two limiting  $C_b$  factors corresponding to an unbraced beam (Eq. 2) and an effectively braced beam (buckling between discrete braces);  $M_{cr}$  is given by Eq 1;  $C_T$  is a top flange loading modification factor:  $C_T = 1.2$  for top flange loading and  $C_T = 1.0$  for centroid loading; and  $\bar{\beta}_T$  is the equivalent effective continuous torsional brace (in-k/radian/in. length) given by,

$$\frac{1}{\bar{\beta}_T} = \frac{1}{\bar{\beta}_b} + \frac{1}{\beta_{sec}} \quad \text{and} \quad \beta_{sec} = 3.3 \frac{E t_w^3}{h 12} \quad (5)$$

where  $\bar{\beta}_b$  = stiffness of the attached continuous brace,  $\beta_{sec}$  = cross-section web stiffness per unit length of the beam,  $t_w$  = thickness of web and  $h$  = distance between flange centroids.  $\beta_{sec}$  accounts for cross-section distortion.  $\bar{\beta}_T$  is less than the smallest of  $\bar{\beta}_b$  and  $\beta_{sec}$ . Web stiffeners can be used to increase  $\beta_{sec}$  (Yura, 1993). If the effective brace stiffness is very small, Eq. (4) converges to Eq. 1. If the unbraced length is long, Eq 4 will be dominated by the bracing term. Note that there is no beam length variable in the bracing term. The bracing stiffness requirement in AISC (2005) is based on Eq. 4 with the first term under the radical neglected and  $M_T$  set to the required design strength. When the torsional stiffness of the brace itself is substantial,  $\bar{\beta}_T = \beta_{sec}$  from Eq.5. Loaded pallets in contact with the top flange of unstiffened support beams would represent such a case. Eq. 4 was developed for single curvature loading conditions. Studies undertaken on restrained beams indicated that some

minor adjustments and clarifications were necessary for design. When the bracing system is continuous,  $C_{bb}$  is undefined. In such cases, setting  $C_{bb} = C_{bu}$  in Eq. 4 gave good results. It was also determined that correlations with FEA were improved for reverse-curvature, top flange loading cases if the  $C_T$  term was placed outside the radical in Eq. 4. With these substitutions,  $M_T$  is given as:

$$M_T = \frac{C_{bu}}{C_T} \sqrt{M_{cr}^2 + \beta_T EI_y} \quad (6)$$

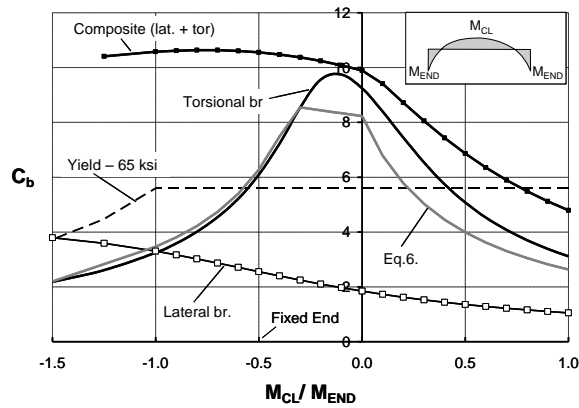


Fig. 8. Bracing Types on Top Flange

A comparison of Eq. 6 and FEA results is given in Fig. 8. The FEA results shown by the dark solid curve without markers were for a 20 ft long beam restrained at both ends and no twist at the top flange. This loading condition was the most critical case for lateral bracing alone discussed previously. For comparison, the FEA lateral bracing results from Fig. 7 are reproduced and shown by the open circle markers. For

$M_{CL}/M_{END} > -1.0$ , torsional bracing provides greater capacity than lateral bracing. The results from Eq. 6 shown by the solid gray line compare favorably with the FEA results. The dashed line in Fig 8 shows the yield limit state (65 ksi) for the W16×26 section. Buckling controls

when  $C_b$  values are below the dashed line. Torsional bracing becomes less effective than lateral bracing for beams with two inflection points for  $M_{CL}/M_{END} < -1.0$ , when the unbraced length of the compression flange at one end  $L_c$  is very small ( $L_c/d < 2$ ). If both lateral movement and twist are prevented at the top flange (curve with solid markers) that is typical in composite construction, yielding will occur before buckling when there are inflection points ( $M_{CL}/M_{END} < 0$ ). Lateral buckling in composite construction is discussed in more detail in the next section.

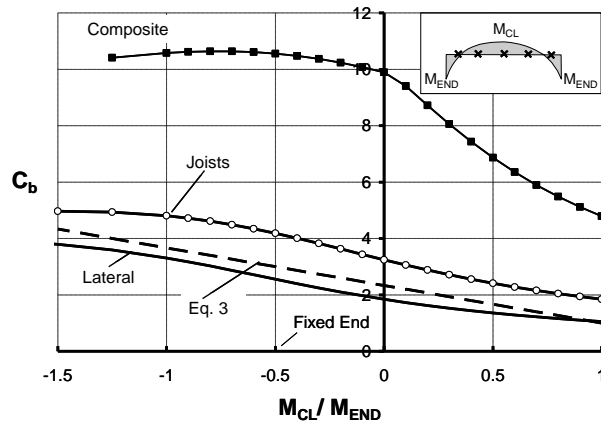


Fig. 9. Typical Joist bracing system

**Joist Systems.** Closely spaced joists that support the roof diaphragm provide equivalent continuous top flange lateral bracing. However, Essa and Kennedy (1995) showed the joists also supply a small amount of torsional restraint. They recommend a minimum rotational restraint of 270 in-k/rad. Using only 0.25 of this value (70 in-k/radian)

combined with zero lateral displacement at the joist locations, the 20 ft beam ( $L/d = 15$ ) restrained at both ends was reanalyzed. Five joists at 4 ft spacing were used with deformations controlled only at those five locations. The results are shown in Fig. 9 by the line with open markers. Recall that for this case with lateral only that Eq. 3 gave some unconservative results as shown in Fig. 7. Those results are reproduced in Fig. 9. The small torsional restraint has a significant effect and Eq. 3 is now shown to be conservative.

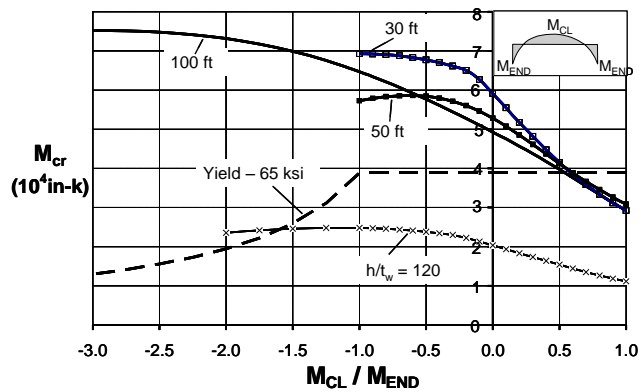


Fig. 10. Composite Beams – Effect of Length and Web Slenderness

## COMPOSITE BEAMS

When lateral displacement and twist of the top flange are prevented, the classic lateral-torsional buckling strength equation (Eq. 1) is no longer valid. The buckled shape is dominated by distortion of the web so is often called distortional buckling instead of lateral-torsional buckling. Solutions presented by Johnson (1985), Williams et al(1993) and Linder, J. (1998) have shown that web slenderness,  $h/t_w$ , is the dominant factor affecting lateral buckling, not unbraced length. This behavior is illustrated in Fig 10 by the FEA results for a W40×149 that has the highest  $h/t_w$  (59.3) of all W

shapes.  $M_{cr}$  for three different span lengths, 30, 50 and 100 ft, are shown in the upper portions of the figure. For uniform compression along the entire length of the unbraced bottom flange ( $M_{CL}/M_{END} = 1.0$ ),  $M_{cr}$  is similar for all three lengths. There is some separation among the three curves for moment diagrams with inflection points, i.e. negative  $M_{CL}/M_{EN}$ . The solutions for the 30 and 50 ft lengths have been terminated at  $M_{CL}/M_{EN} = -1.0$  because of web shear buckling from the very high applied loads. The largest  $M_{cr}$  was achieved with the 100 ft beam. The plastic moment limit for 65 ksi steel is shown by the dashed line so yielding will control rather than buckling except when there is compression along the entire length of the bottom flange. Lateral buckling can control if the web thickness of the 100 ft long W40×149 is reduced by 50 percent ( $h/t_w = 120$ ) as shown by the curve with (x) markers.

Most previous solutions for composite construction cited earlier were in a graphical or tabular form and not easily suited for standard design. A conservative lateral buckling solution for beams with twist and lateral movement prevented at the top flange,  $M_{TB}$ , is given by,

$$M_{TB} = C_{bT} \sqrt{\frac{EI_y \beta_{sec}}{C_T}} = 13900 C_{bT} \sqrt{\frac{I_y t_w^3}{h}} \quad (7)$$

$$C_{bT} = 1.7 \left( 2 - \frac{M_{CL}}{M_{END}} \right)^{0.7} \leq 4.0 \quad (8)$$

Eq. 7 was obtained from Eq. 4 by ignoring the  $M_{cr}$  term, setting  $\bar{\beta}_T = \beta_{sec}$  and replacing  $C_{bb}$  with  $C_{bT}$ . The top flange loading factor is  $C_T = 1.2$ .  $C_{bT}$  was developed by comparing the critical moment from FEA with the square root term in Eq. 7 as shown in Fig. 11. Eq. 8 is a lower bound to all the cases, which include beams with one end restrained, both ends restrained and a slender web. For rolled W shapes Eq. 7 can be used to determine the lateral buckling capacity for the rare case when the bottom flange is entirely in compression. For the common situation when there are inflection points, yielding always control so

lateral buckling does not have to be checked. For unstiffened plate girders with  $h/t_w > 60$ , lateral buckling should be checked.

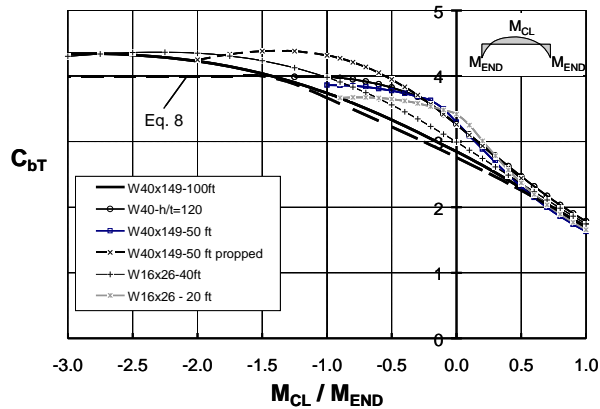


Fig.11.  $C_{bT}$  for Composite Beams

## SUMMARY

Treating the inflection point as a braced point is not recommended since this assumption is unconservative for many commonly encountered problems. The unbraced length that should be utilized in design should be the spacing between points with zero twist. A number of expressions for the moment gradient factor,  $C_b$ , have been presented to account for beams with inflection points and bracing on only one flange. For beams braced on the top flange, torsional bracing is more effective than lateral bracing. Lateral buckling will not occur in composite rolled beams with inflection points. For composite slender webs girders, a conservative solution is provided

## REFERENCES

AISC (1993), *Modern Steel Construction*, Vol. 33, N.6, June, p.10

- AISC (1995), *Modern Steel Construction*, Vol. 35, N.9, Sept., p.10
- AISC(2005), *Steel Construction Manual*, Amer. Inst. of Steel Constr., 13th Ed., Chicago.
- CISC (2003), *Advantage Steel*, Can. Inst. of Steel Constr, N. 7, p. 4
- Essa, H.S. and Kennedy, D.J.L.(1995), "Design of Steel beams in Cantilever-Suspended-Span Construction", *J. of Struct. Engrg*, ASCE, Vol. 121, No. 11, pp. 1667-1673
- Helwig, T.A. and Yura, J.A.(2008), "Shear Diaphragm Bracing of Beams", *J. of Struct. Engrg*, ASCE, Vol. 134, No. 3, pp.348-363.
- Johnson, R.P.(1985), "Continuous Composite Beams for Buildings", *IABSE-ECCS Symposium Report – Steel in Buildings*, Vol. 48, Luxembourg, pp 195-202
- Kirby, P.A. and Nethercot, D.A., (1979), *Design for Structural Stability*, New York, John Wiley & Sons.
- Linder, J. (1998),"Lateral Torsional Buckling of Composite Beams", *J. Constructional Steel Research*, **46: 1-3**, Paper No. 289.
- Nakamura, T. and Wakabayashi, M. (1981), "Lateral Buckling of Beams Braced by Purlins", *Inelastic Instability of Steel Structures and Structural Elements*, U.S. Japan Seminar, Y. Fujita and T.V.Galambos, ed.
- Nethercot, D.A. and Rocky, K.C.(1972), "A Unified Approach to the Elastic Lateral Buckling of Beams", *AISC Eng. J.*, Vol. 9, No. 3, pp. 96-107.
- Timoshenko, S.P. and Gere, J.M. (1961), *Theory of Elastic Stability*, McGraw-Hill, New York.
- Taylor, A.C., and Ojalvo, M., (1966), "Torsional Restraint of Lateral Buckling," *J. of Struct. Engrg*, ASCE, ST2, April, pp. 115-129.
- Williams, F.A., Jemah, A. and Lam, D.,(1993),"Distortional Buckling Curves for Composite Beams", *J. of Struct. Engrg*, ASCE, Vol. 119, No. 7, July, 1993, pp. 2134-2149.
- Yura, J.A. (1987), "Elements for Teaching Load and Resistance Factor Design", AISC, Chicago, IL, 30 pp.
- Yura, J.A. (1993), "Fundamentals of Beam Bracing", *Proc. SSRC Conf., "Is Your Structure Suitably Braced?"* Milwaukee, Apr., 20 Updated: *AISC Eng. J.*, Vol. 38, No. 1, 2001, pp. 11-26.